Liposomal doxorubicin attenuates cardiotoxicity via induction of interferon-related DNA damage resistance

Gyöngyösi, Mariann ; Lukovic, Dominika ; Zlabinger, Katrin ; Spannbauer, Andreas ; Gugerell, Alfred ; Pavo, Noemi ; Traxler, Denise ; Pils, Dietmar ; Maurer, Gerald ; Jakab, András ; Riesenhuber, Martin ; Pircher, Andreas ; Winkler, Johannes ; Bergler-Klein, Jutta

Abstract: AIMS The clinical application of doxorubicin is severely compromised by its cardiotoxic effects, which limit the therapeutic index and the cumulative dose. Liposomal encapsulation of doxorubicin (Myocet®) provides a certain protective effect against cardiotoxicity by reducing myocardial drug accumulation. We aimed to evaluate transcriptomic responses to anthracyclines with different cardiotoxicity profiles in a translational large animal model for identifying potential alleviation strategies. METHODS AND RESULTS We treated domestic pigs with either doxorubicin, epirubicin, or liposomal doxorubicin and compared the cardiac, laboratory and hemodynamic effects with saline-treated animals. Cardiotoxicity was encountered in all groups, reflected by an increase of plasma markers NT-proBNP and Troponin I and an impact on body weight. High morbidity of epirubicin-treated animals impeded further evaluation. Cardiac magnetic resonance imaging with gadolinium late enhancement and transthoracic echocardiography showed stronger reduction of the left and right ventricular systolic function and stronger myocardial fibrosis in doxorubicin-treated animals than in those treated with the liposomal formulation. Gene expression profiles of the left and right ventricles were analysed by RNA-sequencing and validated by qPCR. Interferon-stimulated genes, linked to DNA damage repair and cell survival, were downregulated by doxorubicin, but upregulated by liposomal doxorubicin in both the left and right ventricle. The expression of cardioprotective translocator protein TSPO was inhibited by doxorubicin, but not its liposomal formulation. Cardiac fibrosis with activation of collagen was found in all treatment groups. CONCLUSIONS All anthracycline-derivatives resulted in transcriptional activation of collagen synthesis and processing. Liposomal packaging of doxorubicin induced interferon-stimulated genes in association with lower cardiotoxicity, which is of high clinical importance in anticancer treatment. Our study identified potential mechanisms for rational development of strategies to mitigate anthracycline-induced cardiomyopathy.

DOI: https://doi.org/10.1093/cvr/cvz192

Originally published at:
Gyöngyösi, Mariann; Lukovic, Dominika; Zlabinger, Katrin; Spannbauer, Andreas; Gugerell, Alfred; Pavo, Noemi; Traxler, Denise; Pils, Dietmar; Maurer, Gerald; Jakab, András; Riesenhuber, Martin; Pircher, Andreas; Winkler, Johannes; Bergler-Klein, Jutta (2020). Liposomal doxorubicin attenuates cardiotoxicity via induction of interferon-related DNA damage resistance. Cardiovascular Research, 116(5):970-982.
DOI: https://doi.org/10.1093/cvr/cvz192

ESC European Society of Cardiology
Cardiovascular Research
doi:10.1093/cvr/cvz192

Liposomal doxorubicin attenuates cardiotoxicity via induction of interferon-related DNA damage resistance

Mariann Gyöngyösi [1]*, Dominika Lukovic[1], Katrin Zlabinger[1], Andreas Spannbauer [1], Alfred Gugerell [1], Noemi Pavo [1], Denise Traxler [1], Dietmar Pils [2], Gerald Maurer[1], Andras Jakab[3,4], Martin Riesenhuber [1], Andreas Pircher[5], Johannes Winkler [1], and Jutta Bergler-Klein [1]

[1]Department of Cardiology, Medical University of Vienna, Währinger Gürtel 18-20, 1090 Vienna, Austria; [2]Center for Medical Statistics, Informatics, and Intelligent Systems (CeMSIIS), and Department of Surgery, Medical University of Vienna, Währinger Gürtel 18-20, 1090 Vienna, Austria; [3]Department of Biomedical Imaging and Image-guided Therapy, Medical University of Vienna, Währinger Gürtel 18-20, 1090 Vienna, Austria; [4]Center for MR-Research, University Children's Hospital Zurich, Steinwiesstraße 75, 8032 Zurich, Switzerland; and [5]Division of Hematology and Oncology, Medical University of Innsbruck, Anichstraße 35, 6020 Innsbruck, Austria

Received 19 November 2018; revised 17 April 2019; editorial decision 16 July 2019; accepted 17 July 2019

Time for primary review: 23 days

Aims The clinical application of doxorubicin (DOX) is severely compromised by its cardiotoxic effects, which limit the therapeutic index and the cumulative dose. Liposomal encapsulation of DOX (Myocet®) provides a certain protective effect against cardiotoxicity by reducing myocardial drug accumulation. We aimed to evaluate transcriptomic responses to anthracyclines with different cardiotoxicity profiles in a translational large animal model for identifying potential alleviation strategies.

Methods and results We treated domestic pigs with either DOX, epirubicin (EPI), or liposomal DOX and compared the cardiac, laboratory, and haemodynamic effects with saline-treated animals. Cardiotoxicity was encountered in all groups, reflected by an increase of plasma markers N-terminal pro-brain-natriuretic peptide and Troponin I and an impact on body weight. High morbidity of EPI-treated animals impeded further evaluation. Cardiac magnetic resonance imaging with gadolinium late enhancement and transthoracic echocardiography showed stronger reduction of the left and right ventricular systolic function and stronger myocardial fibrosis in DOX-treated animals than in those treated with the liposomal formulation. Gene expression profiles of the left and right ventricles were analysed by RNA-sequencing and validated by qPCR. Interferon-stimulated genes (ISGs), linked to DNA damage repair and cell survival, were downregulated by DOX, but upregulated by liposomal DOX in both the left and right ventricle. The expression of cardioprotective translocator protein (TSPO) was inhibited by DOX, but not its liposomal formulation. Cardiac fibrosis with activation of collagen was found in all treatment groups.

Conclusions All anthracycline-derivatives resulted in transcriptional activation of collagen synthesis and processing. Liposomal packaging of DOX-induced ISGs in association with lower cardiotoxicity, which is of high clinical importance in anticancer treatment. Our study identified potential mechanisms for rational development of strategies to mitigate anthracycline-induced cardiomyopathy.

* Corresponding author. Tel: +43-1-40400-46140; fax: +43-1-40400-42160, E-mail: mariann.gyongyosi@meduniwien.ac.at

Keywords Anthracyclines • Cardiotoxicity • DNA damage response • Large animal model • Liposomal doxorubicin • RNA-seq

Graphical Abstract

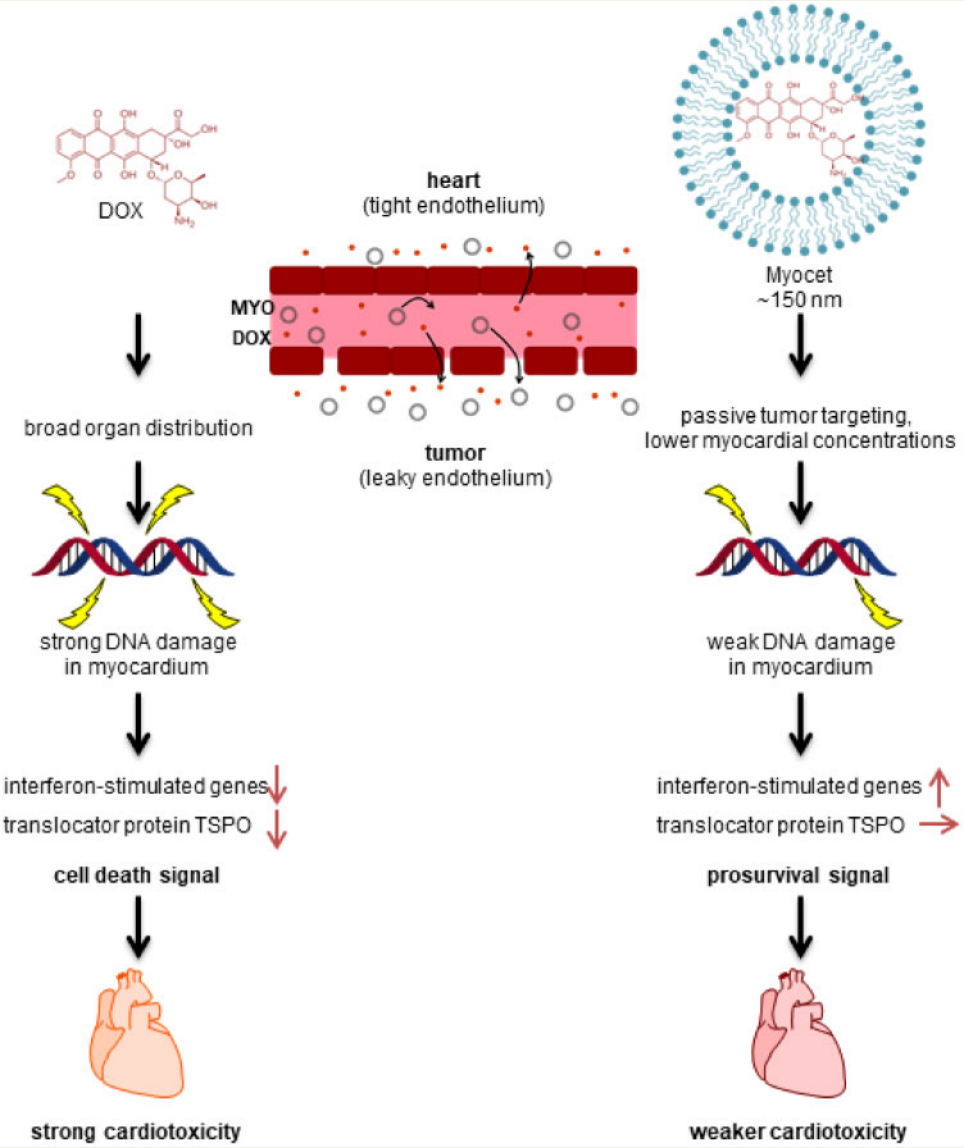

1. Introduction

The 5- to 10-year survival rates of patients suffering from certain tumours, such as breast, haematologic, or childhood cancers exceed 80%. This is mainly due to refined therapy by chemotherapeutics, such as anthracyclines, immunotherapies, other specific treatments, and/or targeted tumour excision or irradiation.[1] Unfortunately, 10–75% of cancer survivors suffer from chronic health issues in later life, including heart failure, vascular or valve diseases, and other cardiac complications, caused by toxicity of many chemotherapeutics.[2] Anthracyclines are one of the most frequently used anticancer drugs. Recent data of a study in adult cancer patients showed that the majority of cardiovascular toxicity, defined as a decrease of left ventricular (LV) ejection fraction (EF), occurred within the first year after the completion of doxorubicin (DOX) chemotherapy.[3] The development of cardiotoxicity correlates with the cumulative anthracycline dose. Clinical studies and the ESC guidelines suggest that early detection and eventual treatment of heart failure of patients exposed to anticancer agents might allow for a partial or complete recovery of LV dysfunction and positively impacts cardiac outcome.[4,5] The treatment usually includes an angiotensin-converting enzyme-inhibitor and further adjuvant therapies against heart insufficiency. An inverse relationship has been found between the time to cardiac treatment and clinical outcome in cancer patients.[4]

Current means to mitigate anthracycline-induced cardiotoxicity are limited.[5] On the molecular level, the cytostatic effect of anthracyclines is attributed to DNA intercalation, DNA binding and cross-linking,

inhibition of topoisomerase II, and induction of apoptosis. Cardiomyocyte damage is caused by oxidative stress, generation of reactive oxygen species (ROS), inhibition of nucleic acid synthesis, and decreased expression of contractile proteins.[6] In small animal models, cardiotoxicity was mediated by topoisomerase-IIβ (Top2b).[7] Cardiomyocyte-specific depletion of Top2b protected mice from DOX-induced heart failure. In pigs, transcriptional activation of several matrix metalloproteinases was found after DOX administration.[8] It has been shown that DOX triggers several signalling pathways, such as the MAPK, p53, Jak-STAT, Wnt, MAPK/p53, or PPAR pathways, which might all be involved in DOX-associated cardiomyopathy.[9,10] Proposed strategies for mitigation of cardiotoxicity include iron chelation,[11] VEGF-B gene therapy,[12] stimulation of oxidative phosphorylation,[9] modulation of DNA damage and oxidative stress,[10] or targeting an RNA-binding protein.[13] However, a comprehensive high throughput transcriptomic screening of genes or proteins in a translational large animal model of cardiotoxicity had not yet been performed.

In relation to their therapeutic dose, the cardiotoxicity risks and anticancer outcomes of DOX and its stereoisomer epirubicin (EPI) are similar, because epimerization reduces not only toxicity, but also therapeutic effects.[14] The use of liposomal DOX formulations has reduced cardiotoxicity because of lower myocardial drug concentrations.[14] Liposomes are designed to avoid direct contact of the cytotoxic agent with the vasculature, and influence biodistribution based on leakiness of the endothelium of various organs.[15] Both unPEGylated (Myocet®/MYO) and PEGylated liposomal formulations of DOX (Caelyx®/Doxil®) are in clinical use.

The aim of our study was to investigate molecular mechanisms and impact on gene expression profile of DOX, the liposomal formulation of DOX, Myocet® (MYO), and EPI in a large animal model, to facilitate pharmacological research for cardioprotection during anticancer treatment. Pigs are excellent translational models for investigating cardiac adverse events. The cardiovascular anatomy, physiology, and pathology of pigs compares favourably to that of humans, with the possibility of cardiac imaging with human clinical cameras. Instead of investigation of *a priori* selected transcripts or proteins, we aimed to perform an unbiased approach of global transcriptomic profiling for comprehensive insight into signal transduction pathways and for discovering multiple potential molecular targets[16] and confirmed our findings in *in vitro* cell culture experiments.

2. Methods

2.1 Animal study design

The investigation conforms to the Guide for the Care and Use of Laboratory Animals published by the US National Institutes of Health (NIH Publication No. 85-23, revised 1985). Animal experiments were performed at the Institute of Diagnostic Imaging and Radiation Oncology, University of Kaposvar, Hungary and were approved by the ethics committee (EK: 1/2013-KEATK DOI, MUW §27 Project FA714B0518).

Twenty-three domestic pigs (Sus scrofa, female large whites 30 ± 2 kg, 3 months old) were randomized into four groups receiving either DOX (group DOX, $n = 6$), EPI (group EPI, $n = 6$), Myocet (group MYO, $n = 6$), or physiologic saline (group CO, $n = 5$) in doses equivalent to human treatment regimens (60 mg/m^2 body surface area DOX and MYO, 100 mg/m^2 EPI) as a single 1-h intravenous infusion every 21 days (at Days 1, 22, and 43). Liposomal DOX was prepared directly before the injection according to the manufacturer's instructions. DOX and EPI were dissolved in saline solutions. Pigs were sedated with 12 mg/kg ketamine hydrochloride, 1.0 mg/kg xylazine, and 0.04 mg/kg atropine. An intravenous infusion of the drug or saline was administered via puncture of the femoral vein. Instead of the human equivalent of six treatment cycles, the experiment was terminated early after concluding three cycles, due to the bad health conditions of the surviving animals. After animal inspection, higher mortality was assumed by continuing the treatment, therefore cardiac MRI was performed followed by sacrification of the animals at Day 60. All available samples were included in the respective analyses.

Transthoracic echocardiography (TTE) was performed after each injection to evaluate the systolic and diastolic functions. Blood samples were collected at baseline, after the 1st and before the 2nd and 3rd treatments, and before termination. Before the 1st treatment (Day 1), and 2 weeks after the 3rd infusion (Day 58 ± 1), cardiac magnetic resonance imaging (cMRI) with late enhancement (LE) was performed to assess the right ventricular (RV) and LV systolic cardiac function and fibrosis. For euthanasia, during continuous deep anaesthesia (1.5–2.5 vol% isofluran, 1.6–1.8 vol% O_2, and 0.5 vol% N_2O), an additional dose of intravenous heparin (10 000 U) and 10 mL intravenous saturated potassium chloride (10%) were administered. Hearts were explanted and samples from the left and right ventricles were excised.

2.2 Blood biomarkers

Blood cell counts (numbers of red and white blood cells/RBC, WBC/, platelets) and haemoglobin values were quantified by using Siemens ADVIA 120 equipment. The normal ranges for pigs are 6.0-9.0 10^6/μL for RBC, 10-23 10^3/μL for WBC, 150-450 x10^3/μL for platelets and 110-170 g/L for haemoglobin. Serum creatinine (normal range 20-200 μM/L) and aspartate-aminotransferase (AST, normal range 10-45 U/L) were measured by routine clinical chemical tests. Plasma troponin I (normal value in pigs <0.15 ng/mL), N-terminal pro-brain-natriuretic peptide (NT-proBNP, normal value <136 pg/mL) and creatine kinase (CK, normal range 0–100 U/L) were determined using porcine troponin I type 3, cardiac (CTNI) ELISA (MyBioSource, San Diego, CA, USA), porcine NT-ProBNP ELISA (MyBioSource, San Diego, CA, USA), and porcine creatine kinase ELISA Kits (Abcam, Cambridge, UK).

2.3 cMRI image acquisition and volumetric MRI measurements

We performed cMRI on a 1.5 T Siemens Avanto Syngo B17 scanner (Erlangen, Germany) with a phased-array coil and a vector ECG system. Functional scans were acquired using a retrospective ECG-gated (HR: 80-100 beats/minute), steady-state free precession (SSFP - TRUFISP sequence) technique in short-axis and long-axis views using 1.2 ms echo time (TE), 40 ms repetition time (TR), 25 phases, 50° flip angle, 360 mm field-of-view, 8 mm slice thickness, and 256 x 256 image matrix. For quantitative evaluation of myocardial fibrosis, LE diastolic phase images were obtained after injection of 0.05 mmol/kg contrast medium using an inversion recovery prepared, gradient-echo MRI sequence. Short-axis and long-axis images were obtained 10-15 minutes after gadolinium injection.

Volumetric MRI measurements and visualizations were performed using the software Segment version 1.9 (Medviso AB, Lund, Sweden).[17] We performed semi-automatic segmentation of the LV endocardial and epicardial borders, extending from the most basal short-axis view slice in which the myocardium could be seen in 360 degrees to the most apical slice. Using 3 D volumetry, end-diastolic (EDV), end-systolic volumes

(ESV), global LV EF were automatically calculated on short-axis cine MRI images. EDV and ESV were related to the body weight (EDVi and ESVi).

2.4 Transthoracic echocardiography

Routine TTE was performed at baseline, and during anaesthesia for each infusion treatment. We measured the diameter of the left ventricle from the M-mode of the long-axis parasternal view to assess the global LV systolic function. Pulsed wave Dopplers of diastolic function were recorded by measurements of mitral *E* and *A* waves and the *E*/*e*′ ratio by using 4-chamber view. RV systolic function was assessed by measurement of tricuspid annular plane systolic excursion (TAPSE).

2.5 Histology and immunohistochemistry

LV and RV myocardial samples were stored in formalin, or RNAlater, or fresh frozen. Myocardial samples were stained for fibrosis, ki67, and caspase activity (Supplementary material online).

2.6 Western blot

To assess cleaved (active) caspase 3 activity in the LV of DOX and MYO animals, a quantitative western blot was performed, of 5 DOX and 6 MYO LV samples, in duplicate. Forty micrograms of protein was loaded into each well of a NuPAGE™ 10% Bis-Tris gel. After electrophoresis, the proteins were transferred onto an Immun-Blot® PVDF Membrane (0.45 µm pore size, BioRad). The membrane was cut in half at the 40 kDa marker to stain cleaved caspase 3 (17 kDa) and beta tubulin (50 kDa) separately. The membranes were stained using cleaved caspase 3 Ab (ab13847, Abcam) and beta Tubulin Ab (NB600-936, Novus Biologicals) as loading control. Densitometric analysis was carried out using ImageJ (Rasband, W.S., ImageJ, U.S. National Institutes of Health, Bethesda, MD, USA) by measuring the area under the curve (AUC) of a histogram of each lane in the western blot. The AUC values for caspase 3 were divided by the value of the corresponding loading control to normalize for protein loading.

2.7 Transcriptomic profiling

Detailed methods are described in the Supplementary material online. Briefly, after RNA isolation and enrichment of coding genes by poly(A) selection, libraries were prepared and analysed on an Illumina NGS system with paired-end sequencing. Results were mapped to the pig transcriptome and analysed for statistically significant changes of individual genes and pathways. For investigation of biological relevance, groups were compared and significantly deregulated genes were functionally clustered.

2.8 DOX effects on isolated human cardiomyocytes

Human cardiac myocytes isolated from adult left ventricles (PromoCell, Heidelberg, Germany) were cultured according to the manufacturer's instructions. For gene expression analyses, cells were treated with DOX (6.25 and 1.56 nM) in 48 well plates (2×10^4 cells per well) for 48 h, lysed in Qiazol (Qiagen). RNA was isolated with an RNeasy micro kit followed by cDNA synthesis with a QuantiTect RT kit and qPCR with Sybr Green (all Qiagen) according to the manufacturer's instructions. For cytotoxicity testing, cells were seeded into 96 well plates (10^4 cells per well) and incubated for 24 h in standard cell culture medium. For induction of interferon-inducible genes, poly (I:C) was applied in a concentration of 1 µg/mL, and cells were further incubated for 4 h. DOX was added to pretreated and control cells in concentrations of 10 µM, 1 µM, 400 nM, 100 nM, 25 nM, 6.25 nM and 0.1 nM, and cells were incubated for 48 h. Cytotoxicity was assessed with an EZ4U cell proliferation and cytotoxicity kit (Biomedica, Vienna, Austria), based on the derivatization to a formazan dye, according to the manufacturer's instructions, and absorption was read after 4 h. A second cytotoxicity assay was performed for direct comparison of the effect of DOX and Myocet on cell viability, using the same methods and dosages as described above without poly (I:C) stimulation.

2.9 Statistics

Differences between treatment and control groups were tested for normality with Shapiro–Wilk, and parametric data were evaluated for statistical significance using one-way ANOVA tests with Bonferroni *post hoc* corrections. The Kaplan–Meier survival analysis was calculated for all groups. A difference was considered statistically significant at $P < 0.05$. Data analyses and interpretations were performed by an experienced observer who was blinded to the randomization and to results. Statistical analysis was performed using SPSS 18.0 (SPSS Inc., USA) software, and graphs were prepared in SigmaPlot 13.0 (Systat Software Inc., USA). Sample sizes for all figures are $n = 6$ for DOX and MYO, and $n = 5$ for controls, unless otherwise indicated.

For gene array analysis, to test for all comparisons (i.e. differences between regions of interest: LV and RV in DOX vs. CO and MYO vs. CO) a linear model for each gene was fitted and the estimated coefficients and standard errors for these contrasts were computed.

3. Results

3.1 Study design and survival

Animals of the DOX and MYO groups showed better survival (*Figure 1A*) compared to group EPI. The two surviving EPI animals had obvious symptoms of cardiotoxicity (highly elevated troponin I and NT-proBNP with low LV EF). Due to the insufficient number of surviving animals, the EPI group was excluded from the further analyses. The reasons of premature death were leucopenia and thrombocytopenia (one DOX and two EPI pigs), renal failure (one EPI and one MYO pig), and haemorrhagic perimyocarditis in one EPI animal. Obduction revealed haemorrhagy in the right ventricle and haemorrhagic pericarditis in one DOX and one EPI pig, and pericarditis (two) and haemorrhagic pericarditis (one) in three EPI pigs. All deceased animals in the cytostatic treatment groups had elevated Troponin I and NT-proBNP levels.

3.2 Body weight, biomarkers, and myocardial fibrosis

The weight of the MYO and control pigs was significantly higher after the first treatment until the end of the experiments compared to the pigs in the DOX group, indicating better general health of these animals (*Figure 1B*). Both NT-proBNP and TnI increased during cytostatic treatment and was in pathologic range in all animals of both groups (*Figure 1C, D*). The baseline values of the RBC, WBC, platelet, haemoglobin, AST, and creatinine did not differ between the groups (Supplementary material online, *Figure S1*). A significant drop of the number of platelets was measured in both DOX and MYO groups, while the liver and kidney function parameters increased significantly in both groups.

Blood cell counts showed a mild decrease of red blood cells and platelets before the 3rd and 2nd treatment cycle, respectively. Mild but significant elevation of creatine kinase (CK) was detected in DOX pigs after

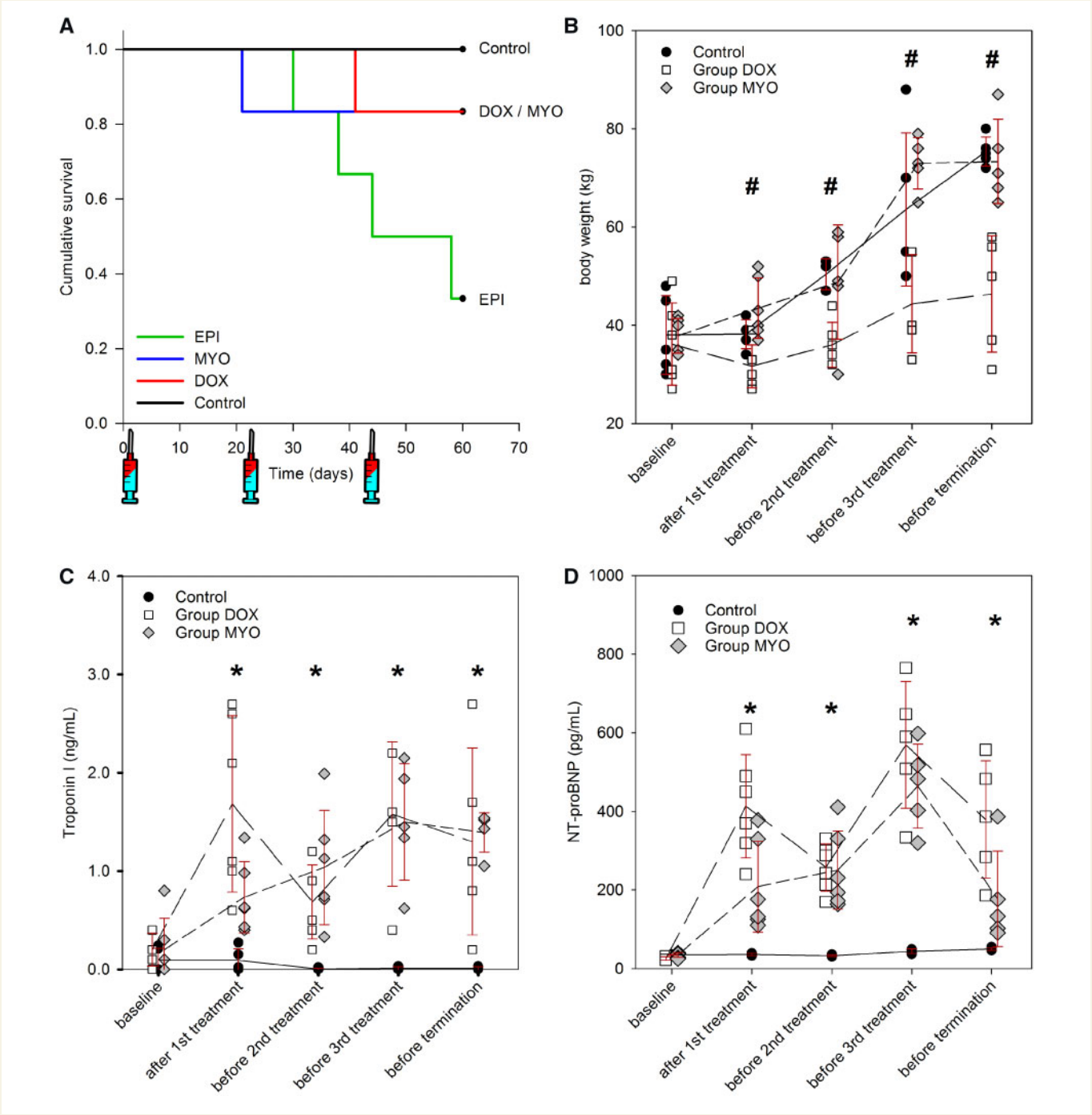

Figure 1 Clinical data of animals treated with doxorubicin (DOX), Myocet® (MYO), or epirubicin (EPI) in comparison to animals treated with physiologic saline infusions (CO). (*A*) Survival: due to low survival rates of epirubicin-treated pigs, they were excluded from further analyses. (*B–D*) Body weight and cardiac markers. The weights of the MYO pigs were significantly higher than those of DOX pigs after the first treatment until the end of the experiments indicating better general health (*B*). Levels of TnI (*C*) and NT-proBNP (*D*) increased during the experiment and were in the pathologic range in all DOX and MYO animals. *$P < 0.05$ CO vs. MYO/DOX, #$P < 0.05$ DOX vs. CO/MYO (ANOVA with Bonferroni *post hoc* test).

the 2nd treatment ($P < 0.05$ in comparison with MYO pigs), which was absent after the 3rd treatment, showing the insensitiveness of CK as a cardiotoxicity biomarker (Supplementary material online, *Figure S1*). Aspartate aminotransferase as a marker for hepatotoxicity also showed a slight increase starting after the first treatment but not during further treatment cycles.

HE and MOVAT staining of the LV and RV samples showed disorientation of muscle fibres in hearts in all three treatment groups (Supplementary material online, *Figure S2*). Picrosirius red staining revealed smaller degrees of LV (6.8 ± 2.1% vs. 8.6 ± 1.4% vs. 11.0 ± 2.0%) and RV (6.5 ± 1.7% vs. 8.7 ± 1.0% vs. 9.1 ± 1.0%) fibrosis of the MYO pigs as compared to the DOX and EPI animals ($n = 6$, $P < 0.05$ MYO vs.

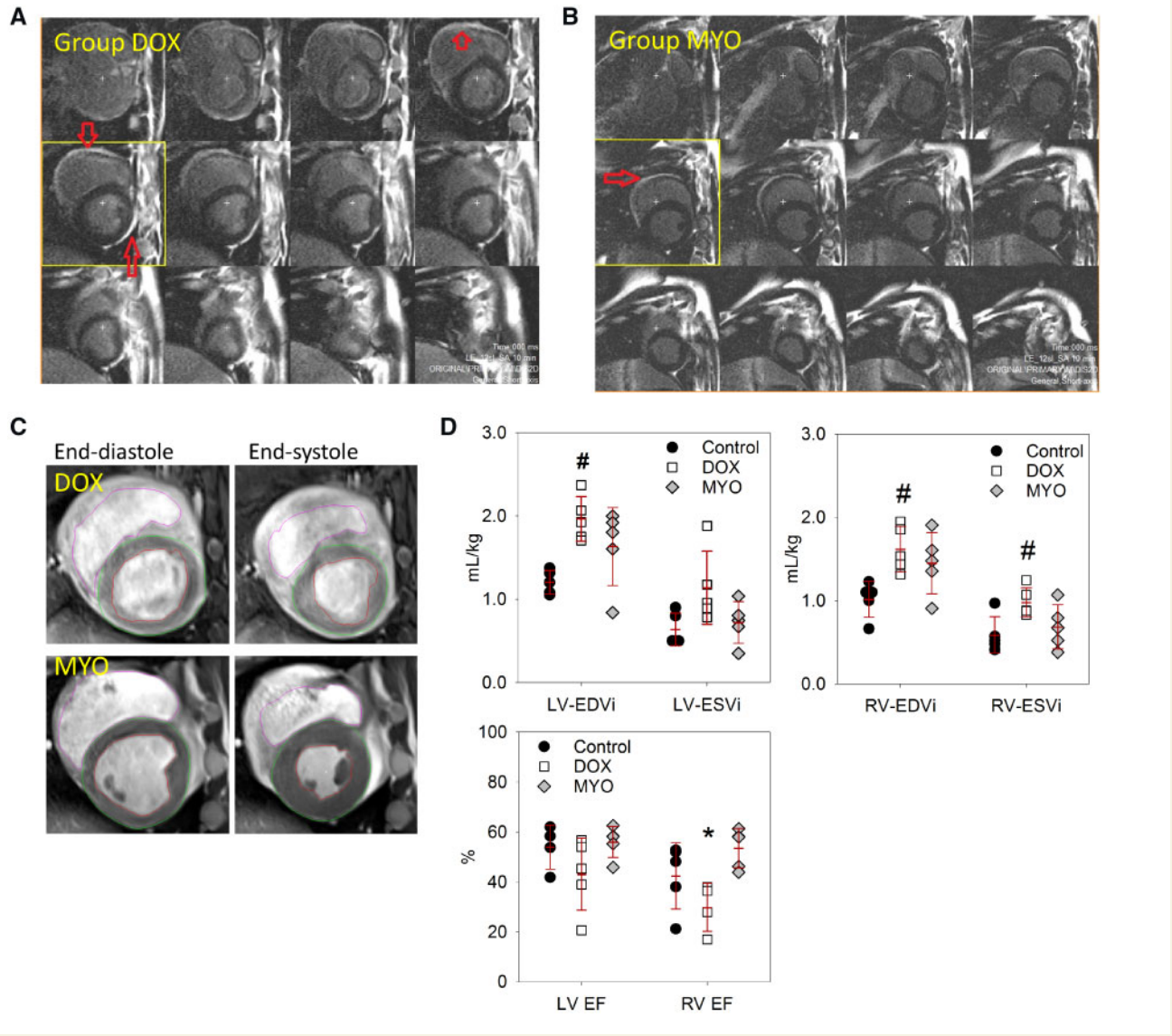

Figure 2 Cardiac fibrosis of pigs treated with doxorubicin (DOX), Myocet (MYO), or physiologic saline (CO). (*A* and *B*) Cardiac magnetic resonance imaging (cMRI) with late enhancement, short-axis view. Animals in both groups showed distinct fibrosis in the right and left ventricle (red arrows). (*C*) Representative short-axis images of the RV and LV of DOX (upper panel) and MYO (bottom panel) animals. Better contraction capacity of animals in Group MYO (bottom panel) as compared with Group DOX (upper panel) with end-diastolic (left) and end-systolic (right) contours of the LV. (*D*) Cardiac function of the pigs related to body weight, assessed by cMRI. LV and RV index (EDVi, end-diastolic volume; ESVi, end-systolic volume, both related to body weight, $n = 5$ for all groups), and function (EF, ejection fraction; $n = 4$ for Control LV and DOX RV, $n = 5$ for others). Group MYO animals presented similar LV and RV function as the Group CO animals. $^{\#}P < 0.05$ DOX vs. CO, $^{*}P < 0.05$ DOX vs. MYO (ANOVA with Bonferroni *post hoc* test).

DOX). Overall, the assessment of cardiac function and histology show that MYO-treated animal developed less severe cardiotoxicity than DOX-treated pigs, although the markers TnI and NT-proBNP were increased in a similar extent.

Supplementary material online, *Figure S2* shows representative histological images of the LV and RV in DOX, MYO, and EPI groups with myocardial tissue fibrosis.

3.3 Systolic and diastolic cardiac function

Baseline LV and RV function was normal in all animals (mean LV EF 62.6 ± 6.2%, LV EDV 62 ± 9 mL, ESV 38 ± 8 mL). Two weeks after the 3rd treatment, cMRI+LE showed that animals in the MYO group had higher RV EF ($P < 0.05$) than those in the DOX group, and we found a trend towards higher LV EF, smaller LV and RV end-diastolic volume index (EDVi) and end-systolic volume index (ESVi) (*Figure 2D*) in the MYO pigs. TTE showed impaired LV diastolic function in DOX, but not MYO animals, and RV systolic dysfunction (*Figure 3*).

3.4 Transcriptomic profiling

PCA, illustrating similarities and variations of complex datasets, shows strongly altered gene expression profiles in LV and RV of DOX and MYO groups compared to CO (Supplementary material online, *Figure*

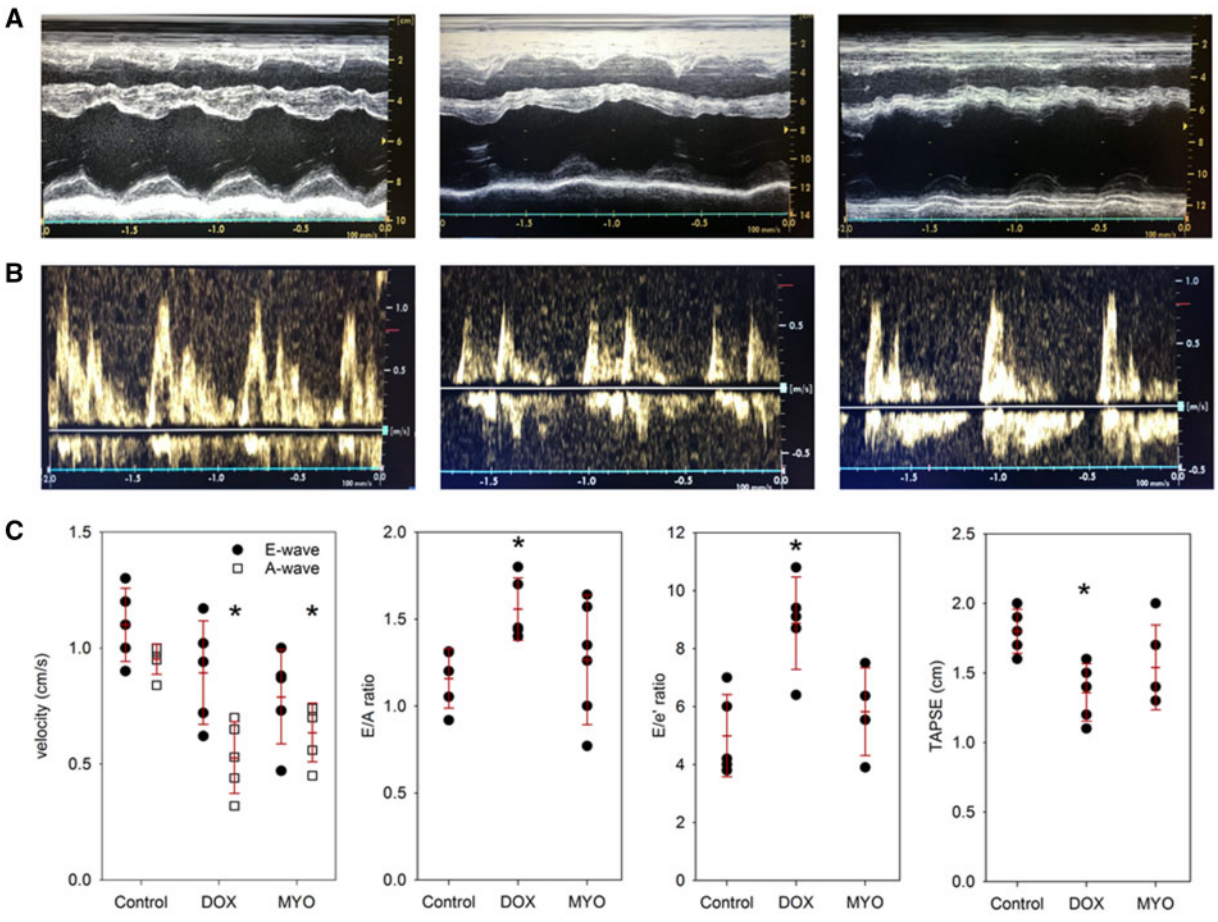

Figure 3 Echocardiographic parameters of the pigs treated with doxorubicin (DOX), Myocet (MYO), or physiologic saline (CO). (*A*) M-mode echocardiography of the left ventricle of CO (left), MYO (mid), and DOX (right) animals. (*B*) Pulsatile Doppler of the mitral valve, for calculation of *E*/*A* ratio of CO (left), MYO (mid), and DOX (right) animals. (*C*) Left ventricular diastolic parameters (*E* and *A* waves and *E*/*e*′ ratio, $n = 5$ for all groups) and tricuspid annular plane systolic excursion (TAPSE, $n = 5$ for CO and DOX, $n = 4$ for MYO) assessed by transthoracic echocardiography. We identified significant differences between the DOX and MYO groups regarding LV diastolic function and RV systolic parameters. *$P < 0.05$ CO vs. DOX/MYO (ANOVA with Bonferroni *post hoc* test).

S3). RV gene expressions of the MYO pigs were slightly closer to controls, while moderate differences between DOX and MYO pigs were identified. Venn diagrams (Supplementary material online, *Figure S4*) reveal considerable overlap (i.e. genes up- or downregulated in both DOX and MYO groups), but also differences in response to either treatment.

3.5 Cardioprotective mechanisms of liposomal DOX

For assessing the mechanistic differences between cardiotoxicity caused by liposomal and free DOX, we compared the respective gene signatures. Functional clusters of dysregulated genes include apoptosis regulation, proto-oncogenes and oncogenes, cellular homeostasis and DNA repair, collagen synthesis, metabolism, and cytoskeleton (*Figure 4* and Supplementary material online, *Table S1*). Additional genes with significant alterations, which could not be allocated to these clusters, are listed in Supplementary material online, *Table S2*.

A direct comparison of gene clusters (*Figure 5* and Supplementary material online, *Table S3*) shows consistently stronger expression of interferon-responsive genes after MYO treatment. In relation to controls, most of these genes are downregulated by DOX, but upregulated by MYO (Supplementary material online, *Figures S5* and *S6*). Interferon-stimulated genes (ISGs) are induced upon certain degrees of DNA damage and can mediate pro-survival signals.[18] Among those genes, we found altered expression between DOX and MYO of IFIT1 and 2, ISG15, OAS2, and Poly(ADP-ribose)-polymerases (PARP) 1, 9, and 14. PARP 1 and other family members are important mediators of DNA repair, and link cytostatic damage to autophagy and survival mechanisms.[19] Interferon and ISGs are biomarkers for immune response and cell survival after DNA damage, and the gene signature reported here appears to be instrumental in the attenuation of cardiotoxicity by Myocet.[20]

Genes mediating direct responses to cell stress (heat shock proteins and transcription factors) were generally upregulated after DOX and downregulated after MYO treatment (*Figure 4*). Several genes of the HSP70 family exhibited this differential expression while other HSPs, including HSPA4, HSPA5, HSPB1, and HSPD1, showed stronger upregulation in the DOX than in the MYO group. Heat shock protein 47/SERPINH1 is a molecular chaperone for collagen, providing a link to

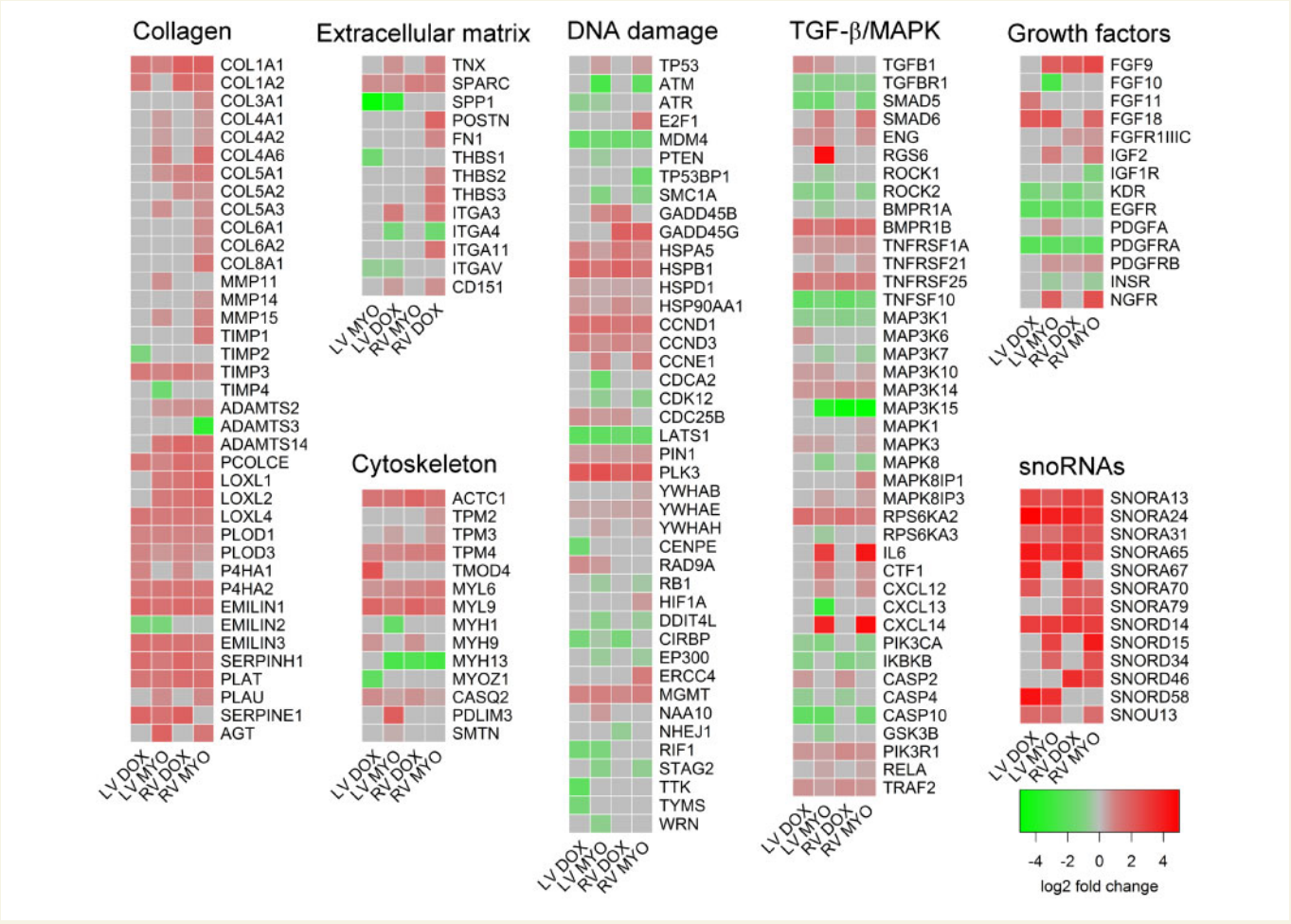

Figure 4 Heat maps of genes relevant for cardiac function of the left (LV) and right ventricle (RV), and cardiomyopathy in doxorubicin (DOX) and Myocet (MYO) treated animals. Genes are functionally grouped into indicated clusters. The heat maps illustrate significant upregulation of collagen and related genes, extracellular matrix and cytoskeleton pathways, genes involved in DNA damage repair, and a less pronounced effect of immune and cell metabolism (transforming growth factor/TGF-beta/and mitogen-activated protein kinase/MAPK/) signalling pathways, regulation of growth factors and small nucleolar RNAs (snoRNA). Significant upregulations are red, downregulations green and non-significant changes grey (all relative to controls, significance for $P < 0.05$, moderated t-statistics adjusted for multiple testing).

fibrosis, and is more strongly upregulated by DOX than by MYO treatment.

Functional clustering identified the translocator protein (TSPO) as a central gene in the responsive network (*Figure 5*), which provides a connection between ISGs (strong expression in MYO) and regulation of transcription (strong expression in DOX). TSPO is abundantly expressed in many tissues and organs, including the heart. Among other functions, it is implicated in apoptosis and cell proliferation and has a protective role in the myocardium.[21] The cardiac expression of TSPO is altered by cellular stress, and it is upregulated in acute stress, but downregulated after repeated injury. Higher expression in the MYO group supposedly contributes to mitigation of cardiotoxicity. To further examine the potential role of TSPO, we stained the protein in LV of DOX and MYO-treated animals (*Figure 6*). A typical mitochondrial punctuate pattern and slightly higher intensity of TSPO staining was found in MYO animals.

Compared to MYO, detection of activated caspase-3 was stronger in DOX tissue samples (*Figure 6*). This indicates higher cytotoxicity and activation of apoptotic pathways caused by higher drug concentrations in the myocardium. The quantitative western blot showed significantly higher cleaved caspase 3 activity in LV samples of DOX than in MYO animals (AUC, DOX vs. MYO: 0.65 ± 0.33 vs. 0.17 ± 0.11 ($P < 0.05$) (*Figure 6*).

3.6 Regulation of gene expression related to collagen production and fibrosis

We also focused on the expression of genes previously associated with anthracycline toxicity (Supplementary material online, *Figure S8*). We detected a strong impact on genes implicated in collagen production and disposition after anthracycline treatments (*Figure 4*).[22] Among those, a profound increase of the transcription of collagens and enzymes for collagen maturation, stabilization, and cross-linking was found, including components of the highly abundant cardiac collagens I and III. COL1A1 and COL1A2 were activated more strongly in the DOX than in the MYO group, while COL3A1 showed significant induction only in the RV of MYO. In histological samples, stronger collagen deposition was found in DOX samples (*Figure 6*). In addition, genes that are involved in collagen

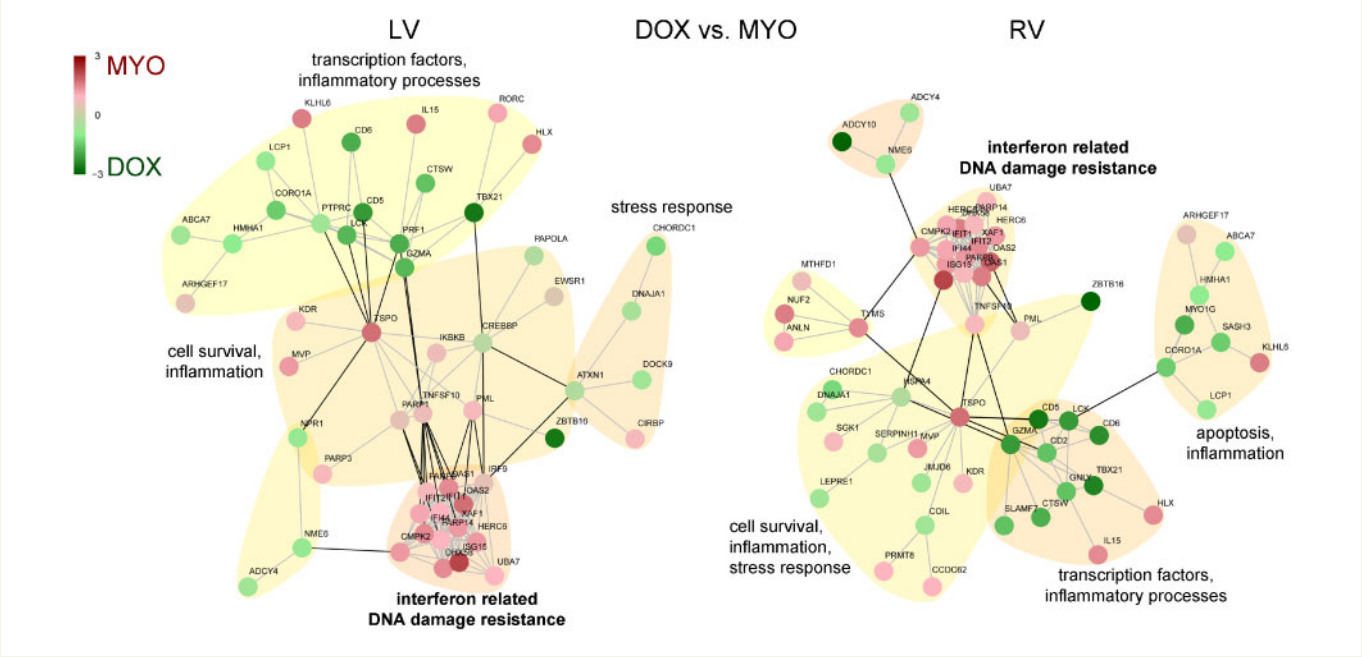

Figure 5 Protein–protein interactions of differentially expressed genes between MYO and DOX groups in the left (LV) and right ventricle (RV). A cluster of interferon-responsive genes was strongly upregulated by MYO treatment. Relative to controls, this cluster was upregulated in MYO, but downregulated in DOX animals. Interferon-inducible genes are upregulated upon DNA damage, and linked with pro-survival and tumour drug resistance. MYO upregulated several PARP (Poly [ADP-ribose] polymerase) genes, which play an important role in DNA damage repair, and are activated by interferon. Likewise, the mitochondrial translocator protein (TSPO), which has a cardioprotective and inflammation-limiting effect, was significantly repressed by DOX compared to controls, while its expression was retained after MYO treatment. In addition, DOX showed stronger induction of genes involved in transcriptional and inflammatory regulation, apoptosis and stress response. Overall, MYO treatment resulted in activation of pro-survival genes, while DOX induced genes involved in cell death and apoptosis. Considerable overlap of gene expression signatures between LV and RV was found.

processing and extracellular matrix remodelling were significantly upregulated. These include procollagen peptidase enhancer PCOLCE, the plasminogen converting enzymes tPA (PLAT) and uPA (PLAU) and its inhibitor PAI-1 (SerpinE1), matrix metalloproteinases (MMPs)-2, 11, 14, and 15, and tissue inhibitors of metalloproteinases (TIMPs)-1 and 3 (*Figure 4*). Enzymes that catalyze collagen cross-linking (lysyl oxidases LOXL1-4, lysyl hydroxylases PLOD1 and 3, and transglutaminase TGM2), folding (proline hydroxylases P4HA1 and 2, and elastin microfibril interlacer Emilin) were also transcriptionally activated. Matricellular proteins thrombospondin-1 and 2, tenascin-C and X, osteopontin, osteonectin (SPARC), periostin, and fibronectin are known to be upregulated during reparative cardiac fibrosis.[11] However, anthracyclines did not induce persistent and complete activation of this group of proteins. However, SPARC was upregulated in all anthracycline groups, and tenascin-C was upregulated in DOX treated animals. Interestingly, we found strongly reduced osteopontin (SPP1) expression[23] in DOX and MYO animals in the LV, but not in the RV.

Overall, these data show a strong induction of cardiac fibrosis, both in the DOX and MYO groups. Collagen 1 and a number of collagen-regulating genes (SerpinE1 and H1, P4HA1, and PLOD3) were more strongly induced after DOX treatment.

3.7 Regulation of cellular homeostasis, inflammation, and signalling pathways

We found deregulation of several genes implicated in response to DNA damage, and apoptosis (*Figure 4*). Among those, the heat shock proteins HSP27 (HSPB1) and HSP60 (HSPD1), which are protective against apoptosis and maintain mitochondrial function, are overexpressed. In contrast, kinases ATM and ATR, activated after DNA double strand breaks and stalled DNA replication, were unchanged or even downregulated. Their downstream target, the central guardian against genomic mutations, TP53, was slightly upregulated only in MYO. The p53 inhibitor MDM4 was reduced after anthracycline treatment and several TP53 targets, such as GADD45B and D, or ERAP1 were upregulated (Supplementary material online, *Figure S9*).

We also investigated known signalling pathways of DOX-induced fibrosis (Supplementary material online, *Figure S10*). TGF-β1 was upregulated, while its receptor TGFBR1 showed reduced expression. The downstream signal transducers SMAD was changed non-significantly, except for a downregulation of SMAD5. Neither the MAP-kinase nor the PI3/Akt pathways were consistently induced in the DOX and MYO groups.

Transmembrane integrin receptors mediate cellular adhesion to the ECM and activate distinct signal transduction pathways. Integrins are generally dysregulated in fibrotic myocardium, with the expression of their individual subtypes varying in different specific cardiomyopathies.[24] Integrins α-1, 3, 5, and 11 and β-1 and 3 are frequently linked to fibrosis in response to MI, pressure overload, or ageing in animal models. We found slight upregulation of the α-3 and α-5 subunits in the MYO and DOX group, respectively, without changes of α-1, α-11, and β-1; β-3 was not detected in the data set. Subunits β-4 and 7 with lesser documented roles in cardiac fibrosis were found to be upregulated, but in

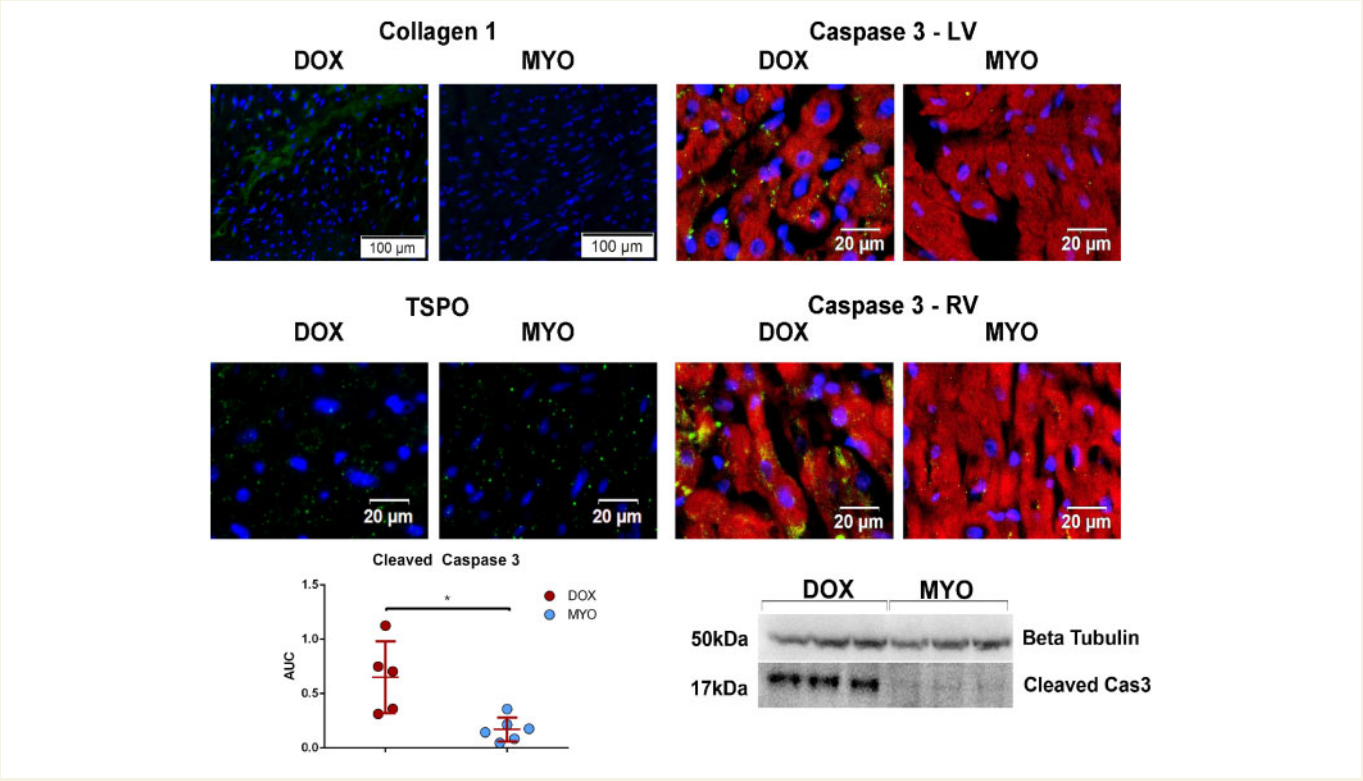

Figure 6 Immunohistochemistry (IHC) and immunofluorescence (IF) analyses of collagen 1, TSPO, and activated caspase-3 with western blot for quantification of apoptosis in LV cross sections of pigs treated with either doxorubicin (DOX) or Myocet (MYO). Representative pictures show stronger interstitial collagen deposition after DOX treatment. Blue, DAPI staining of nuclei; red, actin stained by phalloidin; green, respective protein stained by antibody. Intracellular localization of TSPO is similar in both groups, with a distinct punctuate pattern indicative for mitochondrial localization, with higher signal intensity in MYO group (green). Bottom row: Representative image of western blot of cleaved caspase-3 and tubulin as loading control, with significantly higher caspase-3 activity in DOX as compared to MYO samples. *$P < 0.0$. Scale bars: 50 µm (IHC), 100 µm (IF), and 20 µm (caspase-3).

total no clear and significant transcriptional activation of integrins was detected. The transmembrane proteoglycan syndecan-1, but not other syndecans, was upregulated in both LV and RV of treated animals. In AngII induced fibrosis, syndecan-1 mediates profibrotic signalling through TGF-β/SMAD signalling.[25]

Several fibroblast growth factors were upregulated, with the strongest effect on FGF-9 and 18. We found consistent upregulation of insulin growth factor binding proteins (IGFBP)-6 and 7, the latter of which has been linked to heart failure in a clinical study[26] and is regulated by DOX via p53 activation in tumour cell lines.[27] IGFBPs are modulating IGF effects in tissues and may thus serve as a link between anthracycline induced DNA damage and cardiac fibrosis and heart failure.

Quantitative PCR of selected genes was performed to verify the NGS data. All genes showed differential regulation equivalent to the NGS (Supplementary material online, *Figures S11–S18*).

Besides genes with well-documented roles in cardiac myopathies and in DNA damage response (*Figure 4*), we found dysregulation of a number of genes with previously undocumented role in the myocardium (Supplementary material online, *Table S4*). Several of those are incompletely characterized in Sus scrofa databases and some might be of interest for further investigations. Several small nucleolar RNAs (snoRNAs) were strongly and uniformly upregulated in both LV and RV of DOX and MYO animals. snoRNAs are non-coding transcripts that guide nucleotide modifications of other RNAs. Several members of each the H/ACA box class, which guides the conversion of uridines to pseudouridines, and the C/D box class, which guide 2′-O-methylations, were affected. Recently, some snoRNAs have been linked to oxidative stress caused by DOX,[28] and the activation in our experiment may represent a new mechanism for cardiotoxicity.

3.8 Pharmacokinetics

Plasma concentrations upon application of liposomal DOX were 6- and 14-fold higher than after infusion of the free drug directly after completion of the first infusion, and 10 min later, respectively (*Figure 7A*), indicating faster clearance of the free drug compound. Even 2 weeks after the final dose, residual DOX concentrations were detected in left and right ventricles. As expected, liposomal DOX resulted in lower myocardial concentrations. These results confirm the comprehensive pharmacokinetic data collected during pre-clinical and clinical development of Myocet,[29,30] and the translational value of the pig study.

3.9 Concentration-dependent DOX effects on human cardiomyocytes *in vitro*

To further investigate the involvement of an interferon response in DOX cytotoxicity, we treated human cardiomyocytes with increasing DOX non-lethal concentrations and found a significantly increased

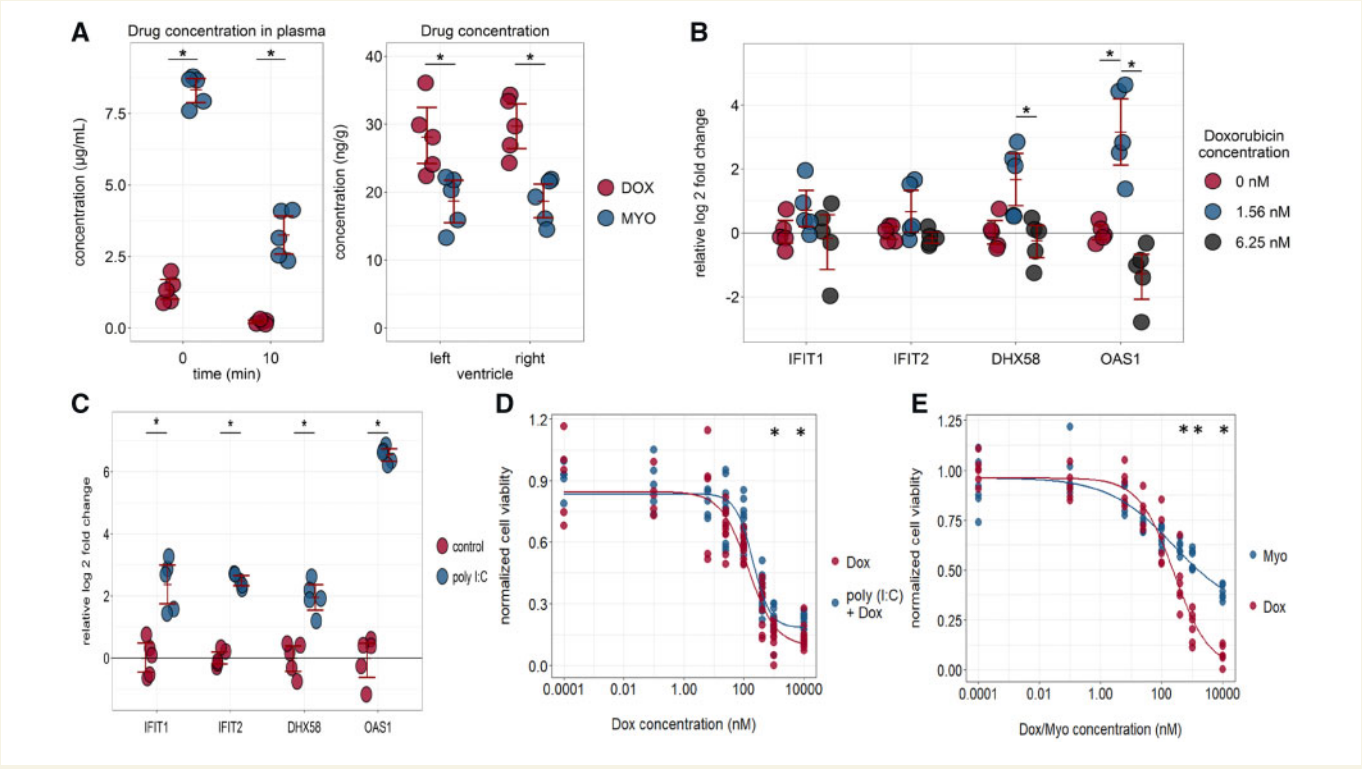

Figure 7 Doxorubicin pharmacokinetics and *in vitro* effects on interferon-responsive genes and cell viability. (*A*) Doxorubicin concentrations in plasma and heart tissue of pigs were analysed by UPLC-MS after application as free drug (DOX) or as liposomal formulation (MYO). Ten minutes after the end of the 1-h infusion, higher drug concentrations were found after treatment with MYO, which were subsequently reduced more slowly than after application of the free drug (DOX), indicative of lower clearance, and slower distribution to cardiac tissues. Two weeks after the third and final treatment cycle, the drug concentration in myocardial samples was still lower after application of MYO compared to DOX. (*B*) Human cardiomyocytes were treated *in vitro* with doxorubicin in sublethal concentrations, and the effect on expression of selected interferon-inducible genes, which were upregulated in porcine hearts *in vivo* by MYO, but not DOX, was assessed. Expression of DHX58 and OAS1 was induced by 1.56 nM DOX, but not by higher concentrations. (*C*) Induction of an interferon response by treating human cardiomyocytes with poly (I:C), a ligand of Toll-like receptor 3. Strong increase of expression was observed for the selected interferon-responsive genes. (*D*) Significantly increase in viability of human cardiomyocytes after induction of interferon response by poly (I:C) and doxorubicin. (*E*) *In vitro* comparison of 24 h incubation of DOX vs. MYO cytotoxicity. Cell viability diverged at higher concentrations with a significant difference from 1 µM indicating an overall lower cytotoxic effect at higher drug concentrations.*$P < 0.05$.

expression of DHX58 and OAS1 after applying low DOX concentrations (*Figure 7B*). This confirms a concentration-dependent effect on interferon-responsive genes. We next examined whether an interferon response has a direct effect on DOX cytotoxicity on cardiomyocytes. Pre-treatment of cardiomyocytes with the nucleic acid and Toll-like receptor ligand poly (I:C)[31] strongly induced expression of the selected set of interferon-responsive genes (*Figure 7C*), and induced a significant protection against DOX cytotoxicity as assessed by mitochondrial activity (*Figure 7D*) in a short incubation time (48 h) by using a single dose. A second assay directly compared the myocardial cell viability after 24 h of incubation with either DOX or MYO in equivalent concentrations, which showed a similar IC50 but diverging toxicity at higher doses. Significantly preserved cell viability was observed from 1 nM drug concentration in the MYO-treated cell culture, compared to DOX ($P < 0.01$; *Figure 7E*) with similar cell viability curves of the poly (I:C)-stimulated and MYO-treated cells. Taken together, the lower myocardial DOX level by applying MYO and the stronger expression of interferon-responsive genes by a lower tissue drug concentration, the *in vitro* experiment indirectly proves the role of interferon-associated mitigation of cardiotoxicity by MYO.

4. Discussion

In line with the clinical knowledge,[32] liposomal encapsulation of DOX (Myocet®) reduced heart damage compared to the free drug in pigs, evidenced by body weight and LV and RV functional parameters. Liposomes exhibit a distinctly altered biodistribution pattern than the lipophilic small molecule DOX: organ distribution is predominantly influenced by their large size, which reduces accumulation in organs with tight endothelium such as the heart, but increases extravasation into tissues with leaky or fenestrated vessels, such as tumour tissue.[33] In clinical trials, liposomal DOX had a more than five-fold lower clearance and an approximately 10- to 15-fold lower volume of distribution (Vss), indicative of the lower degree of tissue uptake.[30,34] In dogs, peak and overall drug concentrations in the myocardium was 30–40% lower after liposomal DOX application compared to the free compound.[35] Our analyses of drug concentrations in plasma and heart tissue confirmed these data also for pigs. Both for DOX and its liposomal formulations, the cardiotoxicity is dependent upon the cumulative administered dose[36] and the better therapeutic index of liposomal formulations are attributed to a lower heart accumulation while maintaining anti-tumour efficacy.[37]

These alterations in tissue accumulation and in particular the lower C_{max} in the myocardium are responsible for the overall lower toxicity of liposomal DOX in pigs. The encountered expressional alterations may serve as a basis for devising novel cardioprotective strategies against anthracycline toxicity.

The most pronounced difference in the RNA-sequencing analysis is the induction and repression of ISGs by MYO, and DOX, respectively (*Figure 5*). Although best known as a key component of the innate immune response and an antiviral defense mechanism, interferon-inducible genes are being increasingly recognized for mediating cell survival after cytostatic stimuli, including irradiation and anthracycline therapy.[38] It has been shown that anthracyclines activate the innate immune response in concentrations well below cytostatic levels.[39] Higher expression of a set of genes termed interferon-related DNA damage signature is connected with DNA damage resistance after DOX treatment.[40] Together with stronger induction of stress response genes by DOX, we propose a mechanism for mitigation of cardiotoxicity by liposomal encapsulation. The limited peak concentration in the heart results in less severe DNA damage and ROS activation, and consequently, an upregulation of ISGs. Activation of this subset of ISGs, as seen after liposomal DOX treatment, induces a pro-survival cell response. On the other hand, the more profound damage caused by higher cardiac DOX concentrations (after unpackaged application) fails to induce ISGs and drives the cell towards cell death. This is reflected by a more severe impact on expression of collagens and ECM genes as indications of cardiac fibrosis, as well as clinical outcomes. The TSPO is potentially central in linking DNA damage, ROS production, interferon response, and finally fibrosis genes. Because of its complex roles in the innate immune system, the interferon response appears to be difficult to exploit for adjuvant therapy. In contrast, TSPO might be a viable target. TSPO ligands are cardioprotective and limit ischaemia–reperfusion damage.[21] In isolated cardiomyocytes, the TSPO ligands 4′-chlorodiazepam and TRO40303 reduced DOX-induced dysfunction and cell death.[41]

Pharmacokinetic analyses confirmed a lower myocardial concentration of the cytotoxic drug when applied in its liposomal form. This is reflected by lower expression of the apoptosis marker activated caspase-3 in MYO animals (*Figure 7*). *In vitro* experiments on isolated human cardiomyocytes confirmed a concentration-dependent effect on gene expression in sublethal DOX concentrations, with lower concentration activating interferon-inducible genes. Stimulation of interferon through TLR-3 protected cardiomyocytes against acute DOX cytotoxicity. Myocardial cell viability was significantly more preserved after incubation of the cells with MYO, as compared to DOX, thus the *in vitro* data corroborate the results of the *in vivo* study. However, several factors, including involvement of fibroblasts and other cell types, the varying extent and mechanisms of ISG-stimulation, and exposure times to drug levels with subclinical toxicity need to be considered for comparing *in vitro* and *in vivo* models. Importantly, there is no reliable method for detection of chronic toxicity caused by repetitive drug administration in simplified *in vitro* models. Meaningful *in vivo* models with high translational value are essential for adequate assessment of molecular mechanisms of cardiotoxicity.

4.1 Relevant pre-clinical signs of cardiotoxicity and cardiac fibrosis

Of note, treatment of pigs with doses equivalent to human application resulted in significant cardiovascular toxicity in all groups. This finding is in contrast with the generally accepted view that cardiotoxicity is a rare to moderately frequent complication of DOX treatment with an incidence of heart failure between 5% and 48% depending on the cumulative dose.[5,42] In our experiment, the cumulative dose failed to reach this limit, yet all animals experienced elevated TnI, even when signs of clinical heart failure (e.g. congestion, dyspnoea) were absent. Moreover, the animals were healthy at the time of the study start, and lacking conventional risk factors. Their young age suggests increased sensitivity to adverse effects of chemotherapy.

In conclusion, we show a uniform and pronounced upregulation of collagens and genes associated with tissue fibrosis in both LV and RV, and both DOX and MYO groups. Together with impaired cardiac function, these data clearly show that cardiac fibrosis was induced by anthracyclines at an early stage. Although the extent of upregulation of fibrosis-associated genes was lower after Myocet, similar caution and in particular close observation of cardiac function is advisable. Our data suggest that primary prevention of cardiotoxicity may be the right choice for all patients before starting anticancer therapy.

Supplementary material

Supplementary material is available at *Cardiovascular Research* online.

Authors' contributions

M.G. and J.B.-K. designed the study. M.G., K.Z., D.L., A.S., and N.P. performed the pig treatments and clinical analyses. K.Z. performed histological analyses. A.J. recorded and analysed PET-MRI images. D.L., A.G., and D.T. analysed plasma samples. D.L., N.P., D.P., A.P., and J.W. collected, analysed, and interpreted RNA-seq data. D.L. and N.P. performed qPCR analyses. M.G., D.L., G.M., A.J., M.R., A.P., J.W., and J.B.-K. interpreted data. M.G. and J.W. wrote the manuscript. All authors contributed to and approved the manuscript.

Conflict of interest: none declared.

Funding

This work was supported by TEVA ratiopharm, which provided NPL-doxorubicin and an unrestricted grant, but was not involved in the study protocol, data acquisition, data analysis, or the writing of the manuscript.

References

1. Trachtenberg BH, Landy DC, Franco VI, Henkel JM, Pearson EJ, Miller TL, Lipshultz SE. Anthracycline-associated cardiotoxicity in survivors of childhood cancer. *Pediatr Cardiol* 2011;**32**:342–353.
2. Broder H, Gottlieb RA, Lepor NE. Chemotherapy and cardiotoxicity. *Rev Cardiovasc Med* 2008;**9**:75–83.
3. Cardinale D, Colombo A, Bacchiani G, Tedeschi I, Meroni CA, Veglia F, Civelli M, Lamantia G, Colombo N, Curigliano G, Fiorentini C, Cipolla CM. Early detection of anthracycline cardiotoxicity and improvement with heart failure therapy. *Circulation* 2015;**131**:1981–1988.
4. Cardinale D, Colombo A, Lamantia G, Colombo N, Civelli M, De Giacomi G, Rubino M, Veglia F, Fiorentini C, Cipolla CM. Anthracycline-induced cardiomyopathy: clinical relevance and response to pharmacologic therapy. *J Am Coll Cardiol* 2010;**55**:213–220.
5. Zamorano JL, Lancellotti P, Rodriguez Muñoz D, Aboyans V, Asteggiano R, Galderisi M, Habib G, Lenihan DJ, Lip GYH, Lyon AR, Lopez Fernandez T, Mohty D, Piepoli MF, Tamargo J, Torbicki A, Suter TM. 2016 ESC Position Paper on cancer treatments and cardiovascular toxicity developed under the auspices of the ESC Committee for Practice Guidelines: the Task Force for cancer treatments and cardiovascular toxicity of the European Society of Cardiology (ESC). *Eur Heart J* 2016;**37**:2768–2801.

6. Chatterjee K, Zhang J, Honbo N, Karliner JS. Doxorubicin cardiomyopathy. *Cardiology* 2010;**115**:155–162.
7. Zhang S, Liu X, Bawa-Khalfe T, Lu L-S, Lyu YL, Liu LF, Yeh E. Identification of the molecular basis of doxorubicin-induced cardiotoxicity. *Nat Med* 2012;**18**:1639–1642.
8. Goetzenich A, Hatam N, Zernecke A, Weber C, Czarnotta T, Autschbach R, Christiansen S. Alteration of matrix metalloproteinases in selective left ventricular adriamycin-induced cardiomyopathy in the pig. *J Heart Lung Transplant* 2009;**28**:1087–1093.
9. Deus CM, Zehowski C, Nordgren K, Wallace KB, Skildum A, Oliveira PJ. Stimulating basal mitochondrial respiration decreases doxorubicin apoptotic signaling in H9c2 cardiomyoblasts. *Toxicology* 2015;**334**:1–11.
10. Thandavarayan RA, Giridharan VV, Arumugam S, Suzuki K, Ko KM, Krishnamurthy P, Watanabe K, Konishi T. Schisandrin B prevents doxorubicin induced cardiac dysfunction by modulation of DNA damage, oxidative stress and inflammation through inhibition of MAPK/p53 signaling. *PLoS One* 2015;**10**:e0119214.
11. Vijay V, Moland CL, Han T, Fuscoe JC, Lee T, Herman EH, Jenkins GR, Lewis SM, Cummings CA, Gao Y, Cao Z, Yu L-R, Desai VG. Early transcriptional changes in cardiac mitochondria during chronic doxorubicin exposure and mitigation by dexrazoxane in mice. *Toxicol Appl Pharmacol* 2016;**295**:68–84.
12. Räsänen M, Degerman J, Nissinen TA, Miinalainen I, Kerkelä R, Siltanen A, Backman JT, Mervaala E, Hulmi JJ, Kivelä R, Alitalo K. VEGF-B gene therapy inhibits doxorubicin-induced cardiotoxicity by endothelial protection. *Proc Natl Acad Sci USA* 2016;**113**:13144–13149.
13. Gupta SK, Garg A, Bär C, Chatterjee S, Foinquinos A, Milting H, Streckfuss-Bömeke K, Fiedler J, Thum T. Quaking inhibits doxorubicin-mediated cardiotoxicity through regulation of cardiac circular RNA expression. *Circ Res* 2018;**122**:246–254.
14. Smith LA, Cornelius VR, Plummer CJ, Levitt G, Verrill M, Canney P, Jones A. Cardiotoxicity of anthracycline agents for the treatment of cancer: systematic review and meta-analysis of randomised controlled trials. *BMC Cancer* 2010;**10**:337.
15. Maeda H. Toward a full understanding of the EPR effect in primary and metastatic tumors as well as issues related to its heterogeneity. *Adv Drug Deliv Rev* 2015;**91**:3–6.
16. Perrino C, Barabási A-L, Condorelli G, Davidson SM, De Windt L, Dimmeler S, Engel FB, Hausenloy DJ, Hill JA, Van Laake LW, Lecour S, Leor J, Madonna R, Mayr M, Prunier F, Sluijter JPG, Schulz R, Thum T, Ytrehus K, Ferdinandy P. Epigenomic and transcriptomic approaches in the post-genomic era: path to novel targets for diagnosis and therapy of the ischaemic heart? Position Paper of the European Society of Cardiology Working Group on Cellular Biology of the Heart. *Cardiovasc Res* 2017;**113**:725–736.
17. Heiberg E, Sjögren J, Ugander M, Carlsson M, Engblom H, Arheden H. Design and validation of segment—freely available software for cardiovascular image analysis. *BMC Med Imaging* 2010;**10**:1.
18. Brzostek-Racine S, Gordon C, Van Scoy S, Reich NC. The DNA damage response induces IFN. *J Immunol* 2011;**187**:5336–5345.
19. Rosado MM, Bennici E, Novelli F, Pioli C. Beyond DNA repair, the immunological role of PARP-1 and its siblings. *Immunology* 2013;**139**:428–437.
20. Cheon H, Borden EC, Stark GR. Interferons and their stimulated genes in the tumor microenvironment. *Semin Oncol* 2014;**41**:156–173.
21. Morin D, Musman J, Pons S, Berdeaux A, Ghaleb B. Mitochondrial translocator protein (TSPO): from physiology to cardioprotection. *Biochem Pharmacol* 2016;**105**:1–13.
22. Gyöngyösi M, Winkler J, Ramos I, Do Q-T, Firat H, McDonald K, González A, Thum T, Díez J, Jaisser F, Pizard A, Zannad F. Myocardial fibrosis: biomedical research from bench to bedside. *Eur J Heart Fail* 2017;**19**:177–191.
23. Kahles F, Findeisen HM, Bruemmer D. Osteopontin: a novel regulator at the cross roads of inflammation, obesity and diabetes. *Mol Metab* 2014;**3**:384–393.
24. Chen C, Li R, Ross RS, Manso AM. Integrins and integrin-related proteins in cardiac fibrosis. *J Mol Cell Cardiol* 2016;**93**:162–174.
25. Lunde IG, Herum KM, Carlson CC, Christensen G. Syndecans in heart fibrosis. *Cell Tissue Res* 2016;**365**:539–552.
26. Barroso MC, Kramer F, Greene SJ, Scheyer D, Köhler T, Karoff M, Seyfarth M, Gheorghiade M, Dinh W. Serum insulin-like growth factor-1 and its binding protein-7: potential novel biomarkers for heart failure with preserved ejection fraction. *BMC Cardiovasc Disord* 2016;**16**:199.
27. Carr CA, Stuckey DJ, Tan JJ, Tan SC, Gomes RSM, Camelliti P, Messina E, Giacomello A, Ellison GM, Clarke K. Cardiosphere-derived cells improve function in the infarcted rat heart for at least 16 weeks—an MRI study. *PLoS One* 2011;**6**:e25669.
28. Holley CL, Li MW, Scruggs BS, Matkovich SJ, Ory DS, Schaffer JE. Cytosolic accumulation of small nucleolar RNAs (snoRNAs) is dynamically regulated by NADPH oxidase. *J Biol Chem* 2015;**290**:11741–11748.
29. Gabizon A, Shmeeda H, Barenholz Y. Pharmacokinetics of pegylated liposomal doxorubicin. *Clin Pharmacokinet* 2003;**42**:419–436.
30. Swenson CE, Bolcsak LE, Batist G, Guthrie TH Jr, Tkaczuk KH, Boxenbaum H, Welles L, Chow SC, Bhamra R, Chaikin P. Pharmacokinetics of doxorubicin administered i.v. as Myocet (TLC D-99; liposome-encapsulated doxorubicin citrate) compared with conventional doxorubicin when given in combination with cyclophosphamide in patients with metastatic breast cancer. *Anticancer Drugs* 2003;**14**:239–246.
31. Li K, Chen Z, Kato N, Gale M, Lemon SM. Distinct poly(I-C) and virus-activated signaling pathways leading to interferon-β production in hepatocytes. *J Biol Chem* 2005;**280**:16739–16747.
32. Xing M, Yan F, Yu S, Shen P. Efficacy and cardiotoxicity of liposomal doxorubicin-based chemotherapy in advanced breast cancer: a meta-analysis of ten randomized controlled trials. *PLoS One* 2015;**10**:e0133569.
33. Wang M, Thanou M. Targeting nanoparticles to cancer. *Pharmacol Res* 2010;**62**:90–99.
34. Mross K, Niemann B, Massing U, Drevs J, Unger C, Bhamra R, Swenson CE. Pharmacokinetics of liposomal doxorubicin (TLC-D99; Myocet) in patients with solid tumors: an open-label, single-dose study. *Cancer Chemother Pharmacol* 2004;**54**:514–524.
35. Kanter PM, Bullard GA, Pilkiewicz FG, Mayer LD, Cullis PR, Pavelic ZP. Preclinical toxicology study of liposome encapsulated doxorubicin (TLC D-99): comparison with doxorubicin and empty liposomes in mice and dogs. *In Vivo* 1993;**7**:85–95.
36. Mitry MA, Edwards JG. Doxorubicin induced heart failure: phenotype and molecular mechanisms. *Int J Cardiol Heart Vasc* 2016;**10**:17–24.
37. Rafiyath SM, Rasul M, Lee B, Wei G, Lamba G, Liu D. Comparison of safety and toxicity of liposomal doxorubicin vs. conventional anthracyclines: a meta-analysis. *Exp Hematol Oncol* 2012;**1**:10.
38. Gasser S, Raulet DH. The DNA damage response arouses the immune system. *Cancer Res* 2006;**66**:3959–3962.
39. Luthra P, Aguirre S, Yen BC, Pietzsch CA, Sanchez-Aparicio MT, Tigabu B, Morlock LK, García-Sastre A, Leung DW, Williams NS, Fernandez-Sesma A, Bukreyev A, Basler CF. Topoisomerase II inhibitors induce DNA damage-dependent interferon responses circumventing Ebola virus immune evasion. *MBio* 2017;**8**.
40. Weichselbaum RR, Ishwaran H, Yoon T, Nuyten DSA, Baker SW, Khodarev N, Su AW, Shaikh AY, Roach P, Kreike B, Roizman B, Bergh J, Pawitan Y, van de Vijver MJ, Minn AJ. An interferon-related gene signature for DNA damage resistance is a predictive marker for chemotherapy and radiation for breast cancer. *Proc Natl Acad Sci USA* 2008;**105**:18490–18495.
41. de Tassigny AA, Assaly R, Schaller S, Pruss RM, Berdeaux A, Morin D. Mitochondrial translocator protein (TSPO) ligands prevent doxorubicin-induced mechanical dysfunction and cell death in isolated cardiomyocytes. *Mitochondrion* 2013;**13**:688–697.
42. Rosa GM, Gigli L, Tagliasacchi MI, Di Iorio C, Carbone F, Nencioni A, Montecucco F, Brunelli C. Update on cardiotoxicity of anti-cancer treatments. *Eur J Clin Invest* 2016;**46**:264–284.

Translational perspective

Although treatment of pigs with doxorubicine, epirubicine, and liposomal encapsulation of doxorubicin (Myocet) with doses equivalents to human application resulted in mild to severe cardiovascular toxicity in all animals, Myocet reduced the cardiac damage evidenced by better left and right ventricular functional parameters measured by cardiac MRI, and less myocardial apoptosis and fibrosis. Pharmacokinetics resulted in lower myocardial concentration of the chemotherapeutic drug after administration of Myocet, compared to doxorubicine. Deep sequencing analysis revealed activated interferon-responsive genes associated with pro-survival signals by Myocet both in right and left ventricular myocardium, which explain the reduced cardiotoxicity on a molecular level.